

Signaling Aptamers for Monitoring Enzymatic Activity and for Inhibitor Screening

Razvan Nutiu, Jasmine M. Y. Yu, and Yingfu Li*^[a]

We examined fluorescence-signaling aptamers as real-time reporters for quantifying enzyme activities and identifying enzyme inhibitors. The conversion of adenosine 5'-monophosphate (AMP) into adenosine by alkaline phosphatase (ALP) was used as a model reaction, and a previously described structure-switching signaling DNA aptamer^[1] was employed as a model reporter. The signaling aptamer, which has a higher affinity for adenosine than for AMP,^[1,2] is able to generate a two-leg signaling profile. The first leg of the signal is produced upon addition of AMP and indicates the formation of a reactant-aptamer complex. The second leg is produced upon addition of ALP and reports the enzymatic conversion of the reactant into the product.

Aptamers are single-stranded nucleic acids with ligand-binding capabilities that can be isolated from random-sequence nucleic acid pools.^[3-7] Several reports have been published that describe the use of fluorescence-based signaling aptamers^[1,8-14] or signaling ribozymes and deoxyribozymes^[15-23] to detect small molecules and proteins in solution. We recently described a strategy for preparing signaling DNA aptamers that function by a mechanism involving coupled structure switching and fluorescence dequenching.^[1] Signaling aptamers usually display signals of great magnitude (more than tenfold fluorescence increase upon target binding) and are capable of real-time reporting at low temperatures (15–37°C). These properties led us to speculate that structure-switching signaling aptamers might be used as sensitive probes to report enzyme-mediated reactions in real time.

Take a simple chemical reaction $A \rightarrow B$ as an example. For a signaling aptamer to be useful for reporting this chemical transformation in real time it must exhibit a different level of fluorescence in the presence of A than with B. If the signaling aptamer has a higher level of fluorescence in the presence of B, the A-to-B transformation can be monitored conveniently by following the increase in the fluorescence intensity of the signaling aptamer. If an enzyme mediates the chemical reaction, the presence of the fluorescent aptamer reporter should permit real-time monitoring of the activity of the enzyme, as well as screening for small-molecule inhibitors.

We found previously that the structure-switching ATP reporter shown in Figure 1 A is able to generate signals with different fluorescence intensities depending on whether adenosine or one of its 5'-phosphorylated analogues is used as the target.

[a] R. Nutiu, J. M. Y. Yu, Prof. Y. Li

Departments of Biochemistry and Chemistry, McMaster University

1200 Main Street West, Hamilton, L8N 3Z5, Ontario (Canada)

Fax: (+1) 905-522-9033

E-mail: liyng@mcmaster.ca



Supporting information for this article is available on the WWW under <http://www.chembiochem.org> or from the author.

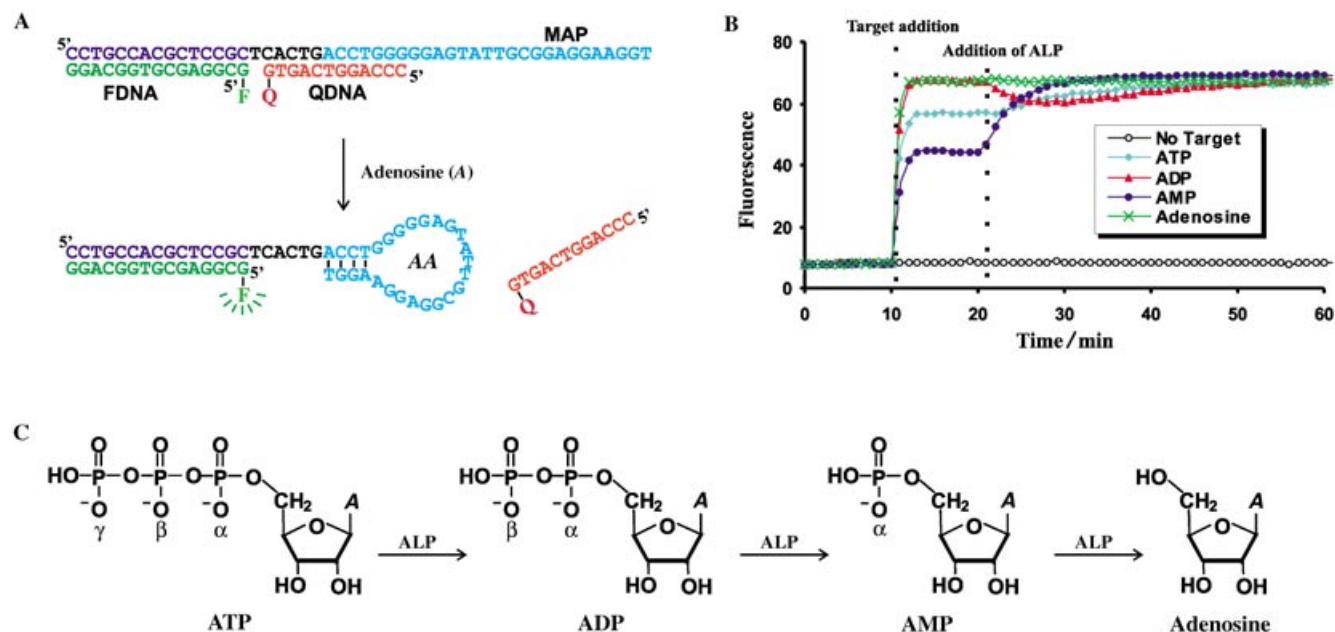


Figure 1. An anti-ATP signaling aptamer and its ability to distinguish adenosine, AMP, ADP, and ATP. A) DNA sequences used for construction of the structure-switching signaling aptamer and the mechanism of signal generation. Two adenosine molecules are shown in the aptamer–target complex in accordance with the structure of the DNA aptamer as determined by NMR spectroscopy (see ref. [14]). B) The two-leg signals observed with the reporter system. The first leg is observed upon addition of each target (final concentration, 0.75 mM), and the second upon addition of calf intestine ALP (1 unit enzyme in 500 μ L solution). Details are given in the Experimental Section. C) Dephosphorylation of ATP by ALP. FDNA, fluorophore-DNA; QDNA, quencher-DNA; MAP, aptamer.

Upon addition of 750 μ M adenosine, AMP, adenosine 5'-diphosphate (ADP), and adenosine 5'-triphosphate (ATP), the intensity of the fluorescence emission from the signaling aptamer increased 8.1, 5.3, 8.3, and 6.9-fold, respectively, compared to the background reading (Figure 1B, each target was added after the signaling aptamer mixture had been incubated for 10 min, as indicated by the first dashed line). These results are consistent with the affinity profiles observed by Kennedy and co-workers in affinity chromatography experiments with the same aptamer as the stationary phase.^[24] These observations led us to speculate that the signaling aptamer is a suitable reporter for nucleotide-dephosphorylating enzymes such as alkaline phosphatase, which is known to remove the 5'-phosphate groups from ATP, ADP, and AMP to convert each of these species into adenosine (Figure 1C).

ALP was added to each target/aptamer mixture 10 minutes after addition of the target (Figure 1B, second dashed line). ALP addition did not cause any intensity change in the adenosine solution (green crosses) or the solution lacking all the adenosine analogues (black empty circles). This result was expected since no chemical reaction occurred in these solutions. ALP promoted a rapid fluorescence intensity increase in the AMP solution (filled dark blue circles). This increase indicates the generation of adenosine, for which the aptamer has a higher affinity than for AMP. The ALP-promoted intensity change in the ADP solution (filled red triangles) was most intriguing: the intensity initially decreased, then slowly returned to the original level. Since ADP contains two phosphate groups (α and β phosphates), two dephosphorylation reactions should occur (see Figure 1C) upon addition of ALP. The initial intensity drop is consistent with the removal of the β -phosphate group (gen-

eration of AMP from ADP, coupled with fluorescence intensity decrease). The eventual intensity recovery is the result of AMP accumulation and subsequent removal of the α -phosphate group (generation of adenosine from AMP, coupled with fluorescence enhancement). Addition of ALP to the ATP solution (light blue diamonds) induced a slow fluorescence increase. This result can be explained by the signaling behaviors associated with three dephosphorylation reactions: the removal of the γ -phosphate group from ATP (generation of ADP, accompanied by fluorescence increase), the removal of the β -phosphate group (generation of AMP, accompanied by fluorescence decrease), and the removal of the α -phosphate group (generation of adenosine, accompanied by fluorescence increase). It appears that the fluorescence gain resulting from the first and the third reactions always surpasses the fluorescence loss associated with the second reaction over the entire incubation period. These observations indicate that the ATP reporter can be utilized as a probe to report reactions catalyzed by ALP in real time.

We chose to examine the AMP–aptamer system further to determine whether the ATP reporter can also be used to quantify ALP activity. We first established the AMP concentration that produced the largest signal in response to the AMP-to-adenosine transition (see Figure 1A in the Supporting Information) by determining the fluorescence intensity differential (ΔF , defined as $F_{\text{adenosine}} - F_{\text{AMP}}$) as a function of the target concentration. A bell-shaped curve was recorded with a ΔF peak at target concentrations of around 500–1000 μ M (Figure 1B, Supporting Information).

Next, we studied the signaling responses of the aptamer during the second leg of the signaling profile in the presence

of 0.75 mM AMP and various amounts of calf intestine ALP. We tested seven different amounts of ALP ranging from 10 to 10^{-5} units in progressive 10-fold dilution steps. ALP was added to a 500- μ L solution of the aptamer-AMP complex in the 25th minute of the experiment (see Figure 2A and the Experimental Section for details). We used the results of these tests to determine the signaling rate as a function of the effective ALP concentration (Figure 2B; the x and y axes are both on a logarithmic scale). The signaling rate corresponds to the speed of fluorescence intensity increase in the initial linear signaling phase following ALP addition and was used as a way to measure the

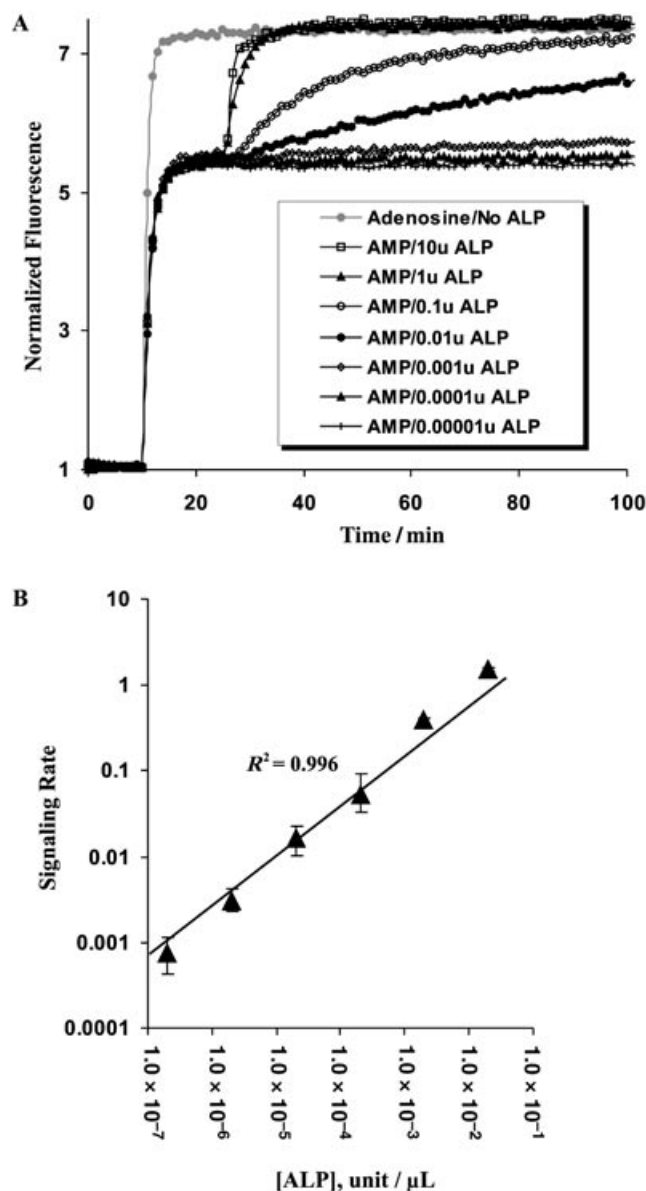


Figure 2. Monitoring the activity of ALP in real time by using a signaling aptamer that reports the occurrence of an AMP-to-adenosine transition. A) Two-leg signaling profiles. The second signal is produced as a result of the addition of calf intestine ALP. ALP was added in various amounts over a range of seven orders of magnitude (the amount of ALP added to each 500 μ L solution is given in the insert). B) Signaling rate versus concentration of ALP. Details are given in the Experimental Section.

enzyme activity. A linear relationship between signaling rate and ALP concentration was observed over an enzyme concentration range covering six orders of magnitude (2×10^{-8} – 2×10^{-3} unit μ L $^{-1}$) with a fixed substrate concentration (the AMP concentration was set at 0.75 mM). These data indicate that the signaling aptamer can be utilized as a sensitive probe for the quantification of effective ALP concentrations.

We also investigated the potential utility of structure-switching signaling aptamers as reporting probes for screening small molecules for enzyme inhibitors. The use of aptamers to establish novel small-molecule screening assays has been demonstrated in two previous studies. Janjic et al. used protein-binding aptamers covalently labeled with a fluorophore.^[25] More recently, Famulok and co-workers designed a fluorescence-signaling allosteric ribozyme system (an aptamer-ribozyme conjugate) to screen for inhibitors of protein enzymes.^[21] We conducted a proof-of-principle, small-molecule screening experiment with our signaling aptamer system. Levamisole and its racemic mixture tetramisole (the chemical structures are shown in Figure 2 of the Supporting Information) are two known inhibitors of porcine ALP (as well as some other mammal ALPs but not calf intestine ALP) that have inhibition constants, K_i , in the low micromolar range.^[26–28] We reasoned that addition of an appropriate amount of levamisole or tetramisole to an anti-ATP signaling aptamer solution containing AMP should attenuate the activity of any porcine ALP added to the mixture. This reduced activity should lead to a slower rate of fluorescence intensity increase in the signaling aptamer solution than was observed in the absence of the inhibitor. Indeed, when levamisole or tetramisole (0.1 mM) was added to a signaling aptamer mixture containing AMP (0.75 mM), the signaling rate showed that the rate of the AMP-to-adenosine conversion promoted by porcine kidney ALP was considerably reduced relative to that of the uninhibited reaction (Figure 3A). Nine other noninhibiting chemical compounds were chosen at random as controls and were tested at the same concentration as the known inhibitors. As expected, no significant rate reduction was observed with these compounds. We performed an inhibition assay on the same eleven compounds in a 96-well plate to demonstrate the feasibility of exploiting structure-switching signaling aptamers for high-throughput screening of small molecules for enzyme inhibitors (Figure 3B). A mixture containing the anti-ATP signaling aptamer, AMP (0.75 mM), and one of the eleven test compounds (0.1 mM) was produced for each well. Two fluorescence readings were taken from each well: the first was recorded when the porcine ALP was added (F_{init}) and the second was recorded 60 minutes later (F_{final}). A control well containing the signaling aptamer and AMP but lacking a test compound was also examined. The inhibitory effect of each compound is represented by the residual activity of the enzyme (percentage activity; Figure 3B) and was calculated as $(F_{\text{final}}/F_{\text{init}})_{\text{compound}} / (F_{\text{final}}/F_{\text{init}})_{\text{control}}$. The results shown in Figure 3B clearly indicate that structure-switching signaling aptamers are suitable for high-throughput screening.

To further verify the reliability of the signaling aptamer system, we used the system to determine the IC_{50} value of levamisole for ALP. We plotted the initial rates of the ALP-cata-

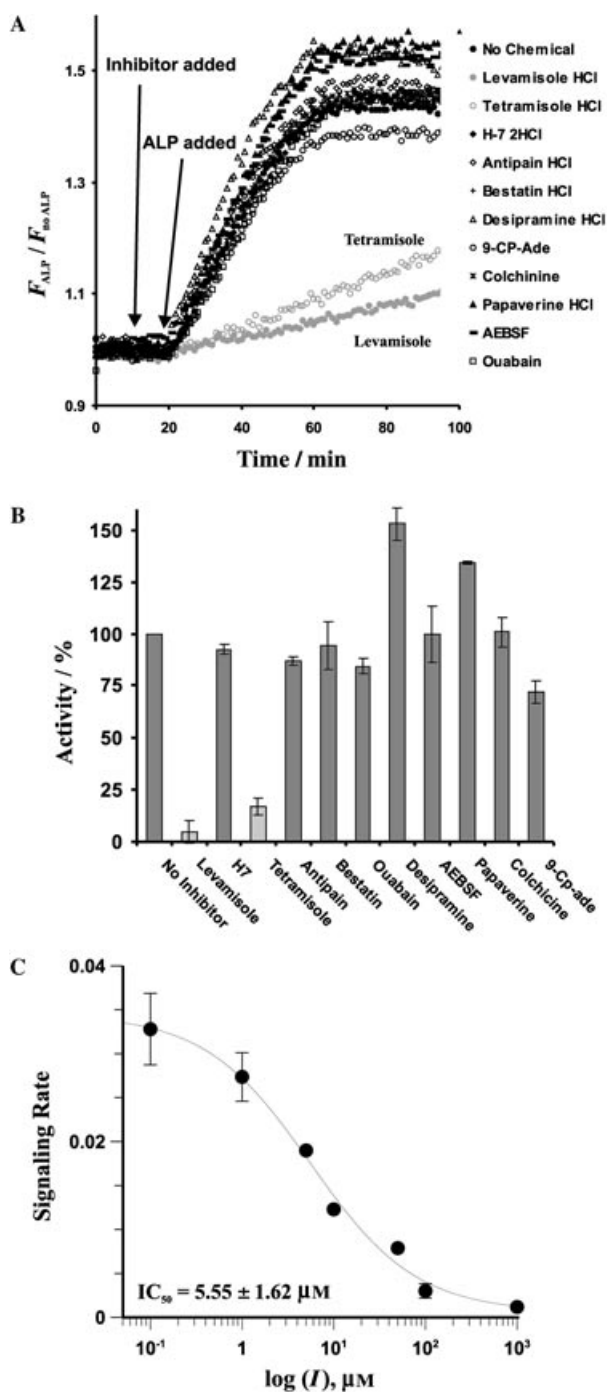


Figure 3. Signaling aptamers as probes for screening small molecules for enzyme inhibitors. A) Real-time monitoring of porcine ALP activity in the presence of various small molecules (including the known ALP inhibitors levamisole and tetramisole) by using the signaling aptamer. B) Inhibition assays performed in a 96-well plate. C) Determination of the IC_{50} value of levamisole for mammal kidney ALP. Details are given in the Experimental Section.

lyzed reaction in the presence of different amounts of levamisole (see the Experimental Section for details) against the concentration of levamisole and obtained a sigmoidal curve from which an IC_{50} value of $5.55 \pm 1.62 \times 10^{-6}$ M was calculated (Figure 3C). We then used the equation $IC_{50} = K_i / [1 + ([S]/K_m)]$ to calculate a K_i value of $8.38 \pm 2.44 \times 10^{-6}$ M for levamisole ([S] is

the concentration of the substrate, 0.75×10^{-3} M; K_m is the Michaelis constant of mammal kidney ALP for AMP, which has been reported as 1.47×10^{-3} M).^[26] This K_i value is in good agreement with that previously reported for mammal kidney ALP with AMP as a substrate (9.86×10^{-6} M).^[26]

In conclusion, we have demonstrated that structure-switching signaling aptamers can be used as real-time reporters of enzyme-mediated chemical reactions. To our knowledge, this is the first study to exploit signaling aptamers as fluorescent reagents for reporting a chemical reaction in real time. We also demonstrated that signaling aptamers can be used as sensitive probes for the quantification of enzyme activities as a result of their large dynamic detection range and very low detection limit. Furthermore, we have shown that structure-switching signaling aptamers are compatible with high-throughput screening technology for the identification and characterization of enzymatic inhibitors.

The signaling aptamer system described herein needs further improvement to achieve better performance and more tests are required to determine its general applicability. For example, although our signaling aptamer system offers a unique, two-leg signaling profile that can be exploited as a built-in checking mechanism to reduce the chance of reporting false positives, the magnitude of the signal in the second signaling leg is relatively small (around 50% increase in intensity compared to the first leg; see Figure 2A and Figure 3A). One possible way to improve the magnitude of the signal is to develop fluorescent aptamers that exhibit a much higher affinity for the product of a given reaction than for the reactant. Such aptamers can be created by using an *in vitro* selection technique through which aptamers are selected for the product as well as against the reactant. At the same time, *in vitro* selection can produce aptamers that have optimum performance at the pH value and metal ion concentration required by the enzyme to enhance the overall performance of the system. Although the anti-ATP signaling aptamer described herein probably distinguishes adenosine from AMP by the difference in charge between the two species, aptamers with the ability to distinguish structurally similar compounds with no charge difference have also been reported.^[29,30] The described assays can, in principle, be applied to any reaction for which a signaling aptamer system that can distinguish the product from the reactant can be established. Our signaling aptamer system involves an assembly of three DNA molecules, FDNA, QDNA, and MAP (see Figure 1A). This type of system offers certain advantages, such as flexibility with regard to fluorophore tagging and system construction,^[1] but an optimization step may be required to determine the most suitable ratio of components.

We used ALP as a model enzyme mainly because it is commercially available and the anti-ATP signaling aptamer can discriminate clearly between adenosine and AMP. Convenient fluorescence-based methods for the detection of ALP activity already exist (see ref. [31–33] for examples) so there is no significant need for an aptamer-based assay for this enzyme. Our efforts will now be directed at exploiting the anti-ATP signaling aptamer to perform screening assays to search for inhibitors of several important enzymes, such as adenosine deaminases

(which transform adenosine into inosine, for which the aptamer has no affinity at all),^[2] adenylyl cyclases (transform ATP into cAMP, for which the ATP aptamer has very low affinity),^[2] or phosphodiesterases (transform cAMP into AMP). New signaling aptamers will also be engineered for targets not related to adenosine and for various metabolic enzymes. It is conceivable that several structure-switching signaling aptamers with different fluorophores or quenchers could be generated through a combination of in vitro selection and signaling aptamer engineering. These aptamers could be used to establish various forms of multiplexed assays for real-time monitoring either of multistep enzymatic reactions or of different enzymatic activities for several reactions occurring in the same solution.

Experimental Section

DNA oligonucleotides and chemical reagents: Both standard and modified DNA oligonucleotides were prepared by automated DNA synthesis with cyanoethyl-phosphoramidite chemistry (Keck Biotechnology Resource Laboratory, Yale University; Central Facility, McMaster University). 5'-Fluorescein and 3'-4-(4-dimethylaminophenylazo)benzoic acid (3'-DABCYL) moieties (in FDNA and QDNA, respectively) were introduced by using 5'-fluorescein-phosphoramidite and 3'-DABCYL-derivatized controlled pore glass (CPG; Glen Research). The products were purified by reversed-phase HPLC. HPLC separation was performed on a Beckman-Coulter HPLC System Gold with a 168 Diode Array detector. The HPLC column was an Agilent Zorbax ODS C18 column (4.5 mm × 250 mm, 5 μm bead diameter). A two-solvent system was used for the purification of all DNA species: Solvent A, 0.1 M triethylammonium acetate (pH 6.5); Solvent B, 100% acetonitrile. The best separation results were achieved with a nonlinear elution gradient (10% B for 10 min, 10–40% B over 65 min) at a flow rate of 0.5 mL min⁻¹. The compound corresponding to the main HPLC peak absorbed very strongly at both 260 nm and 491 nm. The DNA that came off the column within $\frac{2}{3}$ of the peak-width from the centre of the main peak was collected and dried under a vacuum. Unmodified DNA oligonucleotides were purified by 10% preparative denaturing (8 M urea) polyacrylamide gel electrophoresis, followed by elution and precipitation in ethanol. Purified oligonucleotides were dissolved in water and their concentrations were determined spectroscopically.

Calf intestine ALP was purchased from MBI-Fermentas and porcine kidney ALP from Sigma. Both were used without further purification. ATP, ADP, AMP, and adenosine were purchased from Sigma and their solution concentrations were determined by standard spectroscopic methods. All other chemical reagents were obtained from Sigma.

General procedures for fluorescence measurements: The following concentrations of oligonucleotides were used for fluorescence measurements (all DNA sequences are given in Figure 1A): 40 nM for FDNA, 80 nM for the aptamer (MAP), and 120 nM for the quencher (QDNA). The ratio FDNA:MAP:QDNA was set to 1:2:3 to ensure a low background signal. Under these conditions, the vast majority of the FDNA molecules form a duplex structure with MAP and the resulting FDNA–MAP duplexes are able to engage a QDNA molecule for fluorescence quenching. The assay buffer contained NaCl (300 mM), MgCl₂ (5 mM), and tris(hydroxymethyl)aminomethane-HCl (20 mM, pH 8.3). Fluorescence intensities were recorded on a Cary Eclipse fluorescence spectrophotometer (Varian) with excitation at 490 nm and emission at 520 nm. The sample volume was 500 μL in all cases, except for the assay carried out on a 96-well mi-

croplate (150 μL). The measurement of the fluorescence intensities of specific samples is detailed below.

Experimental procedures for Figure 1B: An FDNA–QDNA–MAP signaling mixture (495 μL) in assay buffer was incubated in the absence of any target for 10 min at 22 °C. Adenosine (green crosses), AMP (filled dark blue circles), ADP (filled red triangles), or ATP (filled light blue diamonds) was added to a final concentration of 0.75 mM (achieved by using a 100× stock solution); water was added to the control sample (open black circles). The resulting aptamer/target mixtures were incubated at the same temperature for 10 min. Calf intestine ALP (0.5 units) was introduced (final concentration, 0.001 unit μL⁻¹) and the resultant solution was incubated again for 50 min. A fluorescence reading was recorded every minute. The raw fluorescence data are shown in the figure.

Experimental procedures for Figure 2: The procedures described for Figure 1B were used to obtain the data shown in Figure 2, with three alterations: 1) only AMP (0.75 mM) was used as the target; 2) calf intestine ALP was added in seven different amounts (10⁻⁵–10¹ units; final concentrations, 2 × 10⁻⁸–2 × 10⁻² unit μL⁻¹); 3) the incubation time after the addition of calf intestine ALP was extended to 1200 min. Each experiment was performed in quadruplicate; only one set of data is shown.

We estimated the signaling rate for each solution referred to in Figure 2A by using data taken from within the linear signaling phase of the experiment. Each data series was normalized by using the equation $x = (F - F_0) / (F_{\text{adenosine}} - F_0)$, where $F_{\text{adenosine}}$ is the fluorescence intensity observed with 0.75 mM adenosine, F_0 is the fluorescence reading taken for an AMP-containing solution immediately before calf intestine ALP was added, and F is the fluorescence reading of the same solution at a given time after the ALP addition. Since the AMP-to-adenosine transition is a first-order reaction, x is equivalent to the fraction of AMP that is dephosphorylated by ALP and $(1-x)$ is the fraction of remaining AMP. A plot of $\ln(1-x)$ versus the reaction time should be linear and the negative slope of the line represents the signaling rate. An average signaling rate was calculated for each ALP concentration by using the results of four repeat experiments. Error bars are indicated on the plot.

Experimental procedures for Figure 3A: The ATP reporter and AMP (0.75 mM, 500 μL) were incubated for 10 min at room temperature before a test compound (final concentration, 0.1 mM; the structures of all tested compounds are given in Figure 2 of the Supporting Information) was added. The resulting mixture was incubated for another 10 min, followed by addition of porcine ALP (5 units; final concentration, 0.01 units μL⁻¹) and further incubation for 75 min. The fluorescence intensity (F_{ALP}) was monitored continuously. For each compound, the fluorescence intensity (F_{NoALP}) of a control sample without porcine ALP was also recorded in the same way. Figure 3A shows a plot of $F_{\text{ALP}}/F_{\text{NoALP}}$ versus reaction time for all eleven compounds tested.

Experimental procedures for Figure 3B: The experiment whose results are reported in Figure 3A was performed in duplicate in a 96-well plate (150 μL solution in each well). The concentrations of all components remained the same as those described above. The initial fluorescence intensity (F_{init}) was recorded when porcine kidney ALP was added. The fluorescence intensity (F_{final}) was again recorded 60 min after the addition of ALP. An $F_{\text{final}}/F_{\text{init}}$ value was calculated for each tested compound. The inhibition effect (% ALP activity) was calculated as $(F_{\text{final}}/F_{\text{init}})_{\text{compound}} / (F_{\text{final}}/F_{\text{init}})_{\text{control}}$. The control reaction mixture contained no test compound. Each value plotted is the average of two measurements taken from duplicate

experiments and the error bars represent the difference between the calculated average values and the measured values.

Experimental procedures for Figure 3 C: The same experimental set-up was used as described above for Figure 3 A. The experiments were performed in duplicate with porcine kidney ALP (final concentration, 5 units per 500 μL), AMP (750 μM) as the substrate, and various concentrations of levamisole: 0.1, 1, 5, 10, 50, 100, and 1000 μM . The initial signaling rate was calculated as the slope of the linear portion of a plot of the fluorescent signal after the addition of ALP against ALP concentration. The data were plotted with the GraFit program, which was also used to generate the reported IC_{50} value.

Acknowledgements

We thank the Li laboratory group for insightful discussions. We thank Nadine Elowe and others at the High-Throughput Screening Laboratory at McMaster University for their help regarding the inhibitor screening experiments and Dr. Denis M. Daigle for his advice regarding enzymology. This work was supported by research grants from the Canadian Institutes of Health Research, the Natural Sciences and Engineering Research Council of Canada, and the Canadian Foundation for Innovation. Y.L. is a Canada Research Chair.

Keywords: aptamers • DNA • enzyme inhibitors • fluorescence • small-molecule screening

- [1] R. Nutiu, Y. Li, *J. Am. Chem. Soc.* **2003**, *125*, 4771–4778.
- [2] D. E. Huizenga, J. W. Szostak, *Biochemistry* **1995**, *34*, 656–665.
- [3] C. Tuerk, L. Gold, *Science* **1990**, *249*, 505–510.
- [4] A. D. Ellington, J. W. Szostak, *Nature* **1990**, *346*, 818–822.
- [5] M. Famulok, G. Mayer, M. Blind, *Acc. Chem. Res.* **2000**, *33*, 591–599.
- [6] D. S. Wilson, J. W. Szostak, *Annu. Rev. Biochem.* **1999**, *68*, 611–647.
- [7] S. D. Jayasena, *Clin. Chem.* **1999**, *45*, 1628–1650.
- [8] S. D. Jhaveri, R. Kirby, R. Conrad, E. J. Maglott, M. Bowser, R. T. Kennedy, G. Glick, A. D. Ellington, *J. Am. Chem. Soc.* **2000**, *122*, 2469–2473.
- [9] S. Jhaveri, M. Rajendran, A. D. Ellington, *Nat. Biotech.* **2000**, *18*, 1293–1297.
- [10] N. Hamaguchi, A. D. Ellington, M. Stanton, *Anal. Biochem.* **2001**, *294*, 126–131.
- [11] R. Yamamoto, T. Baba, P. K. Kumar, *Genes Cells* **2000**, *5*, 389–396.
- [12] J. J. Li, X. Fang, W. Tan, *Biochem. Biophys. Res. Commun.* **2002**, *292*, 31–40.
- [13] M. N. Stojanovic, P. de Prada, D. W. Landry, *J. Am. Chem. Soc.* **2001**, *123*, 4928–4931.
- [14] M. N. Stojanovic, P. de Prada, D. W. Landry, *J. Am. Chem. Soc.* **2000**, *122*, 11547–11548.
- [15] A. Jenne, W. Gmelin, N. Raffler, M. Famulok, *Angew. Chem.* **1999**, *111*, 1383–1386; *Angew. Chem. Int. Ed.* **1999**, *38*, 1300–1303.
- [16] K. K. Singh, R. Parwaresch, G. Krupp, *RNA* **1999**, *5*, 1348–1356.
- [17] J. Li, Y. Lu, *J. Am. Chem. Soc.* **2000**, *122*, 10466–10467.
- [18] M. N. Stojanovic, P. de Prada, D. W. Landry, *ChemBioChem* **2001**, *2*, 411–415.
- [19] A. Jenne, J. S. Hartig, N. Piganeau, A. Tauer, D. A. Samarsky, M. R. Green, J. Davies, M. Famulok, *Nat. Biotechnol.* **2001**, *19*, 56–61.
- [20] J. S. Hartig, M. Famulok, *Angew. Chem.* **2002**, *114*, 4440–4444; *Angew. Chem. Int. Ed.* **2002**, *41*, 4263–4266.
- [21] J. S. Hartig, S. H. Najafi-Shoushtari, I. Grune, A. Yan, A. D. Ellington, M. Famulok, *Nat. Biotechnol.* **2002**, *20*, 717–722.
- [22] S. H. Mei, Z. Liu, J. D. Brennan, Y. Li, *J. Am. Chem. Soc.* **2003**, *125*, 412–420.
- [23] Z. Liu, S. H. Mei, J. D. Brennan, Y. Li, *J. Am. Chem. Soc.* **2003**, *125*, 7539–7545.

- [24] Q. Deng, I. German, D. Buchanan, R. T. Kennedy, *Anal. Chem.* **2001**, *73*, 5415–5421.
- [25] L. S. Green, C. Bell, N. Janjic, *Biotechniques* **2001**, *30*, 1094–1096.
- [26] H. Van Belle, *Biochim. Biophys. Acta* **1972**, *289*, 158–168.
- [27] H. Van Belle, *Clin. Chem.* **1976**, *22*, 972–976.
- [28] H. Van Belle, *Clin. Chem.* **1976**, *22*, 977–981.
- [29] A. Geiger, P. Burgstaller, H. von der Eltz, A. Roeder, M. Famulok, *Nucleic Acids Res.* **1996**, *24*, 1029–1036.
- [30] R. D. Jenison, S. C. Gill, A. Pardi, B. Polisky, *Science* **1994**, *263*, 1425–1429.
- [31] B. Rotman, J. A. Zderic, M. Edelstein, *Proc. Natl. Acad. Sci. USA* **1963**, *50*, 1–5.
- [32] W. G. Cox, V. L. J. Singer, *J. Histochem. Cytochem.* **1999**, *47*, 1443–1456.
- [33] S. Avrameas, *J. Immunol. Methods.* **1992**, *150*, 23–32.

Received: January 26, 2004